nilvadipine on RCS rat retinal degeneration by microarray analysis. Biochem Biophys Res Com, 306: 826-831, 2003.

3. Takano Y, et al.: Study of drug effects of calcium channel blockers on retinal degeneration of rd mouse. Biochem Biophys Res Com, 313: 1015-1022, 2004.

33. 色素変性モデルにおけるフォトトランスダクション経路と視細胞死の検討

中尾武史、辻川元一、田野保雄
(大阪大)

研究要旨 網膜色素変性症をはじめとする網膜遺伝性疾患については多くの原因遺伝子が単離されたがその視細胞死にいたるメカニズムは全く不明である。我々は色素変性の患者および、モデルが視物質の局在異常を示すことを手がかりに、これと類似する表現型を示すゼブラフィッシュ変異体 ovl を用いて、フォトトランスダクションが視細胞死に与える影響を検討した。ovl おける視細胞死は暗条件下では明条件下よりも明らかに抑制された。正常視細胞は用いた実験系では視細胞死を示さなかった。これにより ovl 視細胞死には光が促進的に働いていた。ovl においてロドプシン、および Transducinαを発現抑制したところ視細胞死は抑制されたため、この効果はフォトトランスダクション系を介したものと考えられた。次に PDE6 を同様に抑制しても視細胞死は抑制されなかったため、視細胞死のシグナルは Transducin の部位でフォトトランスダクション系につながっていると考えられた。

A. 研究目的

網膜色素変性症は視細胞死を病因の主体とする遺伝性変性疾患群である。遺伝子座異質性が高く、原因遺伝子の多くが単離されたが、視細胞死のメカニズムに関しては不明である。フォトトランスダクション経路は単離された遺伝子の中の大きな部分を占め、また、光毒性の点からも視細胞死との関連を多く言われてきた遺伝子群である。今回の目的は、このフォトトランスダクション経路と視細胞死の関連を vivo のモデルを用いて検討することである。

B. 研究方法

ゼブラフィッシュの ENU 誘導変異体で、視細胞変性モデルである ovl を解析に用いた。ovl は繊毛の輸送蛋白である IFT88 であり ovl はこれを失うことにより外節が発達せず、視物質の局在異常を引き起こし視細胞死に至る。繊毛の蛋白群をコードする遺伝子群は近年、色素変性の原因遺伝子群、とくに、BBS のそれと認識されるに至っている。また、視物質の局在異常は色素変性を含め、視細胞死を引き起こす各種の疾患に認められる病態である。このモデルを用いて視細胞死における光の効果や、フォトトランスダクション経路の視細胞死への影響を vivo で検討した。フォトトランスダクション経路の遺伝子発現抑制には morpholino nucleotide を用い、視細胞の評価は冷凍切片を用い、視細胞マーカーを染色するか、GFP にて Rod を可視化した魚を用い、残存視細胞をカウントすることによった。

（倫理面への配慮）
本研究においては、該当事項はない。

C．研究結果

ovl における視細胞死は光依存性を示した。この光依存性が、フォトトランスダクション経路によるものであることを示すため、抗ロドプシン morpholino を用いてロドプシンの発現を抑制したところ視細胞死が抑制されたことより、フォトトランスダクション系の活性化は視細胞死に促進的に働くことが示唆された。つづいて、このロドプシンからのシグナルがフォトトランスダクションのどの段階で視細胞死を引き起こすのかを検討するため抗 transducin α morpholino を用いて transducin の発現を ovl にて抑制したところ、視細胞死も抑制された。これに対し同様に PDE6 を発現抑制しても視細胞死は抑制されず、よって Transducin の位置で視細胞死のシグナルはフォトトランスダクションと連結していると考えられた。

D．考察

色素変性においてフォトトランスダクションと視細胞死の関連は長年議論されていたが、その詳細なメカニズムについては不明であった。今回、フォトトランスダクションは色素変性状態の視細胞にとってはその視に関して促進的に働くということが示されたことは、重要な知見であると考える。また、その死のシグナルは transducin に結合することも示された。フォトトランスダクション経路は変形された３量体 G 蛋白を中心としたシグナルトランスダクション経路であり、G 蛋白は Gi 型の transducin、共役受容体は Opsin 群、エフェクターは PDE である。ここで、transducin 以降の経路が問題であるのなら、視細胞死のシグナルは比較的選択性の弱いエフェクターか、PDE 以降の cGMP や Ca++が有力なターゲットとなる。

我々はこれらのターゲット経路の一つを薬剤で阻害したところ、ovl での視細胞死は有意に減少した。現在、その他の経路も含め、より特異性の高い化合物や、標的遺伝子の単離を目的としてスクリーニング系を準備している。

E．結論

ovl における視細胞死においてはフォトトランスダクション経路は促進的に働いており、それは transducin において視細胞死のシグナルに連なっていると考えられる。

F．健康危険情報

なし

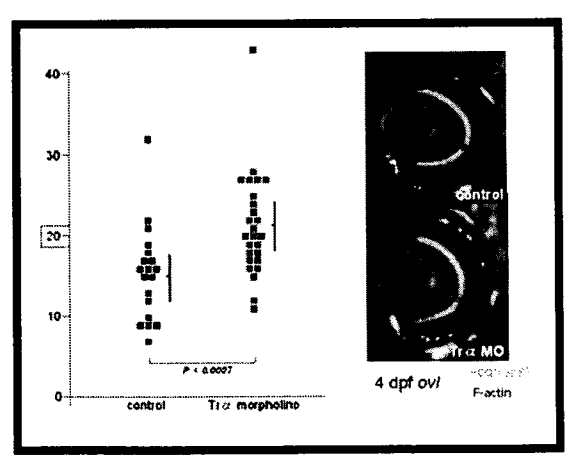

図１transducin 抑制による視細胞死の抑制

G. 研究発表

1. 論文発表

1. Tsujikawa M, Malicki J: Intraflagellar transport genes are essential for differentiation and survival of vertebrate sensory neurons. Neuron.42:703-716, 2004
2. Tsujikawa M, Malicki J: Genetics of photoreceptor development and function in zebrafish. Int J Dev Biol. 48:925-934, 2004
3. Otteson C, Tsujikawa M, Gunatilaka T, Malicki J, Zack D: Genomic organization of zebrafish cone-rod homeobox gene and exclusion as a candidate gene for retinal degeneration in niezerka and mikre oko Molecular Vision 11:986-995, 2005
4. Pujic Z, Omori Y, Tsujikawa M,Thisse B, Thisse C, Malicki J: Reverse genetic analysis of neurogenesis in the zebrafish retina. Developmental Biology 293:330-347, 2006
5. Tsujikawa M, Omori Y, Biyanwila J, Malicki J: Mechanism of positioning the cell nucleus in vertebrate photoreceptors. PNAS. 104:14819-14824, 2007
6. Tsujikawa M, Wada Y, Sukegawa M, Sawa M, Gomi F, Nishida K, Tano Y: Age of onset curves of Retinitis Pigmentosa. Arch Ophthalmol. in press

2. 学会発表

1. Tsujikawa M, Doerre G, Malicki J: Genetic analysis of photoreceptor development. 5th International conference on zebrafish development & genetics. (Medison) 2002/6/13
2. Tsujikawa M., Doerre G,. Malicki J: Characterization of key regulator of photoreceptor development, mikre oko. 3rd European Conference on zebrafish and medaka genetics and development (Paris) 2003/6/13
3. Pujic Z., Tsujikawa M., Thisse B., Thisse C: Reverse genetic analysis of neuro genesis in the retina. 3rd European Conference on zebrafish and medaka genetics and development (Paris) 2003/6/11
4. Tsujikawa M, Malicki J: Ovl is essential for differentiation and survival of vertebrate sensory neurons (Florida) 2004/4/ 26
5. Tsujikawa M, Malicki J:Ovl is essential for differentiation and survival of vertebrate sensory neurons 6th International conference on zebrafish development & genetics (Wisconsin) 2004/8/1
6. Tsujikawa M, Malicki J: mikre oko, a regulator of photoreceptor differentiation. 6th International conference on zebrafish development & genetics (Wisconsin) 2004/8/1
7. 辻川元一、Jarema Malicki: ovl 変異体感覚器受容体における繊毛の喪失と細胞死 第 11 回小型魚類研究会(岡崎)2005 年 9 月 30 日
8. 中尾武史、辻川元一、田野保雄:ゼブラフ

ィッシュ変異体 ovl における視細胞死とフォトトランスダクション　第 111 回日本眼科学会総会(大阪)2007 年 4 月 19 日

9. 辻川元一、ヤレママリッキー:ゼブラフィッシュ視細胞変異体における視細胞死のメカニズム第 111 回日本眼科学会総会(大阪)2007 年 4 月 19 日
10. Nakao T, Tsujikawa M, Tano Y: Phototransduction Accelerates Photoreceptor Cell Death in a Zebrafish Model. The association for research in vision and ophthalmology May 6 2007

H. 知的財産権の出願・登録状況

1. 特許取得

なし

2. 実用新案登録

なし

3. その他

なし

I. 参考文献

なし

Mechanism of positioning the cell nucleus in vertebrate photoreceptors

Motokazu Tsujikawa, Yoshihiro Omori, Janisha Biyanwila, and Jarema Malicki*

Department of Ophthalmology, Harvard Medical School, 243 Charles Street, Boston, MA 02114

Edited by Constance L. Cepko, Harvard Medical School, Boston, MA, and approved July 27, 2007 (received for review January 9, 2007)

Organelles are frequently distributed in a nonrandom manner in a cell's cytoplasm. A particular distribution pattern often facilitates a specific function of a cell, whereas its aberrations can lead to cell death. We show that a mutation in the zebrafish *mikre oko* (*mok*) locus, which encodes dynactin 1 subunit of the dynactin complex, produces a severe displacement of the photoreceptor cell nucleus toward the synaptic terminus. Interference with the function of other dynein complex constituents, including p50/dynamitin, the Lis1 polypeptide, and the disruption of a nuclear envelope component of the *syne* gene family in vertebrate photoreceptors also result in the mispositioning of nuclei. Although the overall photoreceptor polarity is not affected, this phenotype is accompanied by a misdistribution of the Bardet–Biedl syndrome 4 polypeptide and a decreased photoreceptor survival. These findings reveal an important mechanism that regulates nuclear position in vertebrate neurons.

Bardet–Biedl syndrome | retina | motor complex | neurodegeneration

Cell nuclei are precisely positioned in many tissues. In the vertebrate retina and brain, for example, cell nuclei occupy well defined strata, frequently separated from each other by layers of neuronal processes. A mislocalization of nuclei in the context of the vertebrate CNS is likely to result in profound patterning defects and severely compromised function. Genetic defects of nuclear positioning have been characterized in fungi, *Caenorhabditis elegans*, and *Drosophila*. In contrast to invertebrates, nuclear positioning in vertebrate phyla remains poorly characterized. To fill this gap, here we provide genetic analysis of the mechanism that regulates nuclear position in vertebrate photoreceptor cells. To our knowledge, this is the first study of a nuclear localization mechanism in the vertebrate eye and one of very few attempts to understand this process and its significance in the context of the vertebrate nervous system.

Results

***mok* Mutation Causes a Severe Basal Displacement of Nuclei.** A mutation in the *mikre oko* (*mok*) locus results in a rapid loss of nearly all photoreceptor cells by 5 days postfertilization (dpf), one of the most severe photoreceptor defects described in zebrafish so far (1, 2). We showed that in mosaic retinae, $mok^{-/-}$ cells surrounded by wild-type tissue survive markedly longer and develop robust outer segments (2). Photoreceptor morphology is not completely normal, however. Mutant cells retain elongated appearance, but their width is extremely reduced in the central portion of the apico-basal axis, a region normally occupied by the nucleus [Fig. 1*B* (compare with wild-type in Fig. 1*A*)]. This shape change suggests that photoreceptor nuclei are mislocalized. As mok^{m632} photoreceptors die very rapidly during differentiation in homozygous mutant embryos, their phenotype has to be studied in mosaic animals. To determine where nuclei localize in mok^{m632} mutant cells, we visualized them in mosaic retinae, using a nuclear stain (Fig. 1) and evaluated their positions relative to the basal margin of neighboring nuclei (Fig. 1 *A–A″* and *B–B″*, illustrated schematically in Fig. 1*E*). Indeed, mok^{m632} nuclei are severely displaced basally, compared with wild-type ones (Fig. 1*F*, $P < 0.00000007$), and, in the most extreme cases, they translocate into the outer plexiform layer, which in the normal retina consists exclusively of neuronal processes and synaptic termini. Nuclei in another zebrafish photoreceptor mutant ovl^{tz288b} (3) are not mispositioned, indicating that this phenotype is not a general consequence of photoreceptor degeneration [supporting information (SI) Fig. 5 *A–C*]. In addition, mok^{m632} photoreceptor nuclei display a markedly different shape. Although the length of wild-type nuclei along their apico-basal axis equals ≈70% of photoreceptor cell layer thickness, the length of mutant photoreceptor nuclei in the same dimension is only 30% of photoreceptor cell layer thickness [Fig. 1*B* (compare with Fig. 1*A*)]; quantitative estimate in Fig. 1*G*, $P < 0.000002$). The width to length ratio of nuclei is also severely affected by the mok^{m632} defect and equals 0.33 in the wild-type (16 measurements) versus 1.19 in the mutant (10 measurements, $P < 0.0000001$). These observations indicate that mutant nuclei are markedly rounder, compared with wild-type ones.

The correct position of the nucleus on the apico-basal axis of the cell is a major feature of polarity. Does *mok* gene function in other aspects of apico-basal polarity? One conspicuous component of polarity in photoreceptors is the unidirectional transport of billions of opsin polypeptides from the soma into the outer segment (4). An uninterrupted occurrence of this process is a prerequisite for photoreceptor health (3). To investigate whether mok^{m632} mutation affects opsin transport, we stained mosaic retinae with a mix of anti-rod opsin and anti-green opsin antibodies, which recognize ≈40% of photoreceptors. In wild-type environment of mosaic retinae, wild-type photoreceptors ($n = 21$) do not accumulate opsins outside their outer segments (Fig. 1 *C–C″*). Similarly, in mok^{m632} homozygous photoreceptors ($n = 26$), visual pigments localize to outer segments in a manner indistinguishable from wild-type cells, indicating that the mechanism of visual pigment transport is not affected [Fig. 1 *D–D″* (compare with wild type in Fig. 1 *C–C″*)]. To further evaluate whether mok^{m632} outer segments differentiate correctly, we visualized basal bodies of connecting cilia, using anti-γ-tubulin antibodies. Photoreceptor cilia are positioned apically, connecting the outer segment to the rest of the photoreceptor body. We did not find ectopically localized basal bodies in mok^{m632} photoreceptor cells [Fig. 1*I*, $n = 13$ (compare with wild-type cells in 1H, $n = 24$)]. These data indicate that in contrast to nuclear positioning, other key aspects of cell polarity, outer segment formation in particular, are normal in *mok* mutants.

A misplacement of mok^{m632} photoreceptor nuclei may affect the differentiation of synaptic termini, which normally form

Author contributions: M.T. and J.M. designed research; M.T., Y.O., and J.B. performed research; M.T., Y.O., and J.M. analyzed data; and J.M. wrote the paper.

The authors declare no conflict of interest.

This article is a PNAS Direct Submission.

Abbreviations: BBS, Bardet–Biedl syndrome; dpf, days postfertilization; hpf, h postfertilization.

*To whom correspondence should be addressed. E-mail: jarema_malicki@meei.harvard.edu.

This article contains supporting information online at www.pnas.org/cgi/content/full/0700178104/DC1.

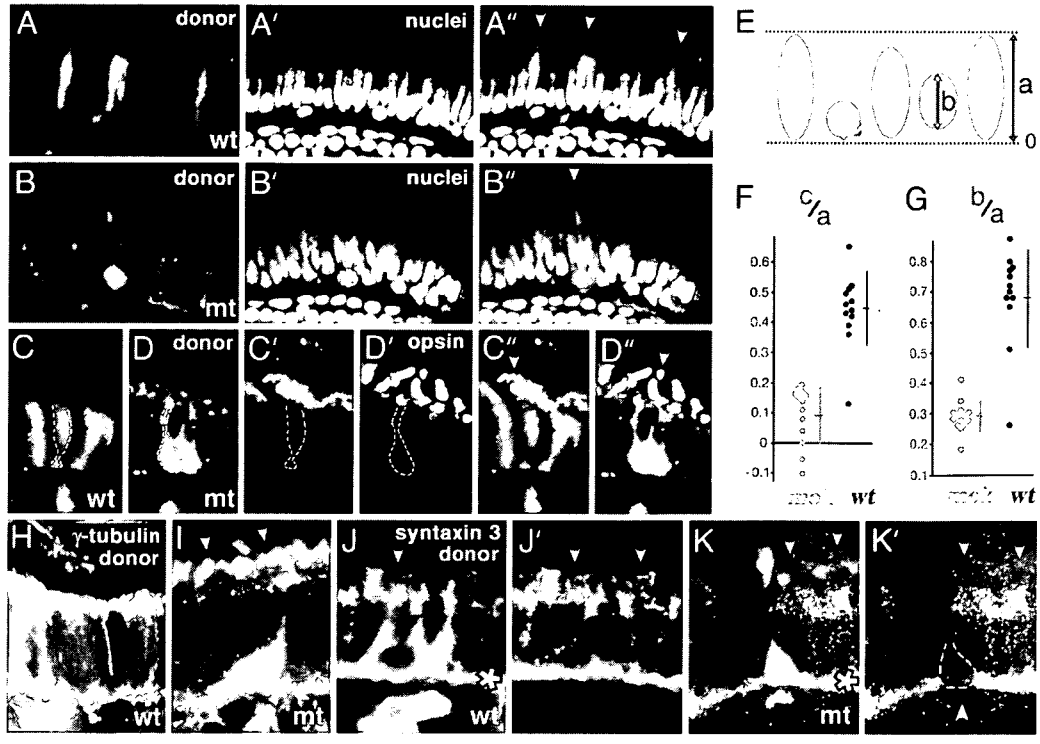

Fig. 1. Nuclear positioning defect in *mok* mutant photoreceptors. All experiments were performed in genetically mosaic retinae. The genotypes of donor-derived cells are indicated in lower right corners. (*A* and *B*) Somata of photoreceptors derived from wild-type (*A*) or mutant (*B*) donors are visualized in red. (*A′* and *B′*) The same sections as in *A* and *B*, stained with YoPro to visualize nuclei. (*A″* and *B″*) Red and green channels shown to the left superimposed. In *A′* and *B′*, the nuclei of donor-derived cells are outlined with white dashes. (*C* and *D*) In contrast to wild-type cells, *mok* photoreceptor nuclei are rounder and displaced basally. Somata of donor-derived wild-type (*C*) and mutant (*D*) photoreceptors surrounded by wild-type cells in mosaic retinae. (*C′* and *D′*) The same sections as in *C* and *D* stained for rod and blue opsins. (*C″* and *D″*) Green and red channels shown to the left superimposed. In wild-type and mutant photoreceptors alike, opsins are confined to outer segments. (*E*) To describe the position of nuclei, we used the following parameters: (*i*) the distance between apical and basal margins of the photoreceptor cell layer; (*ii*) the length of nuclei along the apico-basal axis; and (*iii*) the distance between the center of a nucleus and the basal margin of the photoreceptor cell layer. (*F*) As revealed by their c/a ratios, *mok* nuclei are displaced basally, compared with those in wild-type cells. (*G*) As indicated by the b/a ratios, *mok* nuclei are rounder, compared with those in the wild type. In *F* and *G*, each dot represents a single cell nucleus. Vertical bars and short horizontal cross bars indicate standard deviations and averages, respectively. (*H* and *I*) γ-tubulin staining of basal bodies (yellow) in mosaic retinae, containing wild-type (*H*) and mutant (*I*) donor-derived photoreceptors (in red). In wild-type and mutant donor-derived photoreceptor cells alike, we do not observe basal bodies away from apical cell termini. (*J* and *K*) Syntaxin 3 staining (green) in mosaic retinae containing wild-type (*J*) or mutant (*K*) donor-derived photoreceptor cells (red). (*J′* and *K′*) Syntaxin staining alone. The presence of mutant but not wild-type photoreceptors correlates with discontinuous syntaxin staining (arrowhead in *K′*). In all images, apical termini of photoreceptors and retinal pigmented epithelium are up (indicated with arrowheads). White asterisks in *J* and *K* indicate the outer plexiform layer.

basal to nuclei. To investigate whether this is the case, we stained mosaic retinae with antibodies against syntaxin 3, a component of the photoreceptor synaptic apparatus (Fig. 1 *J* and *K*). In control retinae, syntaxin 3 staining remains uninterrupted in the vicinity of donor-derived wild-type photoreceptor cells (Fig. 1 *J* and *J′*, $n = 11$). By contrast, syntaxin 3 distribution is frequently disrupted in the vicinity of mutant cells (Fig. 1 *K* and *K′*, six of eight cells examined), and we do not observe the characteristic shape of wild-type pedicles in mutant photoreceptors. These results indicate that synaptic differentiation is adversely affected in mutant cells, possibly as a result of nuclear displacement. Synaptic defects may contribute to photoreceptor degeneration in *mok* mutants, although it has to be noted that even severe synaptic defects in *Cacna1f* mutant mice do not cause a marked reduction of photoreceptor viability (5).

***mok* Gene Encodes a Motor Complex Component.** To determine the molecular nature of the *mok* gene product, we performed positional cloning. Conventional linkage analysis confined *mok* to an interval of ≈0.21 cM in the telomeric region of LG7 (Fig. 2*A*). This region contains at least six predicted transcripts, one of which encodes a homolog of the *dynactin 1* subunit of the dynein motor complex, also known as p150. To search for mutations in this gene, we cloned its coding region by RT-PCR and RACE. The ORF of this transcript consists of 1,218 aa and is highly homologous both to the mouse *dynactin 1* (64% identity, 74% similarity) and to its *Drosophila* homolog, *glued* (31% identity, 49% similarity). Both fly and vertebrate proteins contain a microtubule binding domain, a dynein intermediate chain binding domain, and a Bardet–Biedl syndrome (BBS)4 binding domain, which includes a putative ARP-1 binding site (amino acids 955–970; Fig. 2*B* and *SI Text*) (6, 7). *mok* is one of two *dynactin 1* paralogs present in the zebrafish genome. The function of the second gene (*SI Text*), which we term *mok2*, remains at present unknown. Sequence analysis revealed that the mok^{m632} allele contains a nucleotide 2395C → T transition in the *dynactin 1* gene, which results in the appearance of a premature stop codon at the position 799 of the polypeptide. The mutant transcript is expressed at a much lower level, most likely because of nonsense-mediated decay (Fig. 2*C Inset*). To confirm that this mutation is responsible for the mok^{m632} phenotype, we injected anti-*dynactin 1* morpholinos into wild-type embryos. Approximately 60% (7 of 11, SI Fig. 6*A*) of *dynactin 1* morpholino-injected fish display photoreceptor loss at 3 dpf, whereas retinae of control morpholino-treated individuals retain the wild-type phenotype (18 of 18, SI Fig. 6*B*). In parallel, we rescued the mok^{m632} defect by injecting *dynactin 1* mRNA. Mutants treated with GFP mRNA display severe photoreceptor loss, characteristic of mok^{m632} homozygotes (16 of 16, SI Fig. 6*C*). In contrast, the injection of full-length *mok* mRNA rescues photoreceptor loss in 60% (9 of 15, SI Fig. 6*D*) of mutant animals. The injection of either GFP or *dynactin 1* mRNA into wild-type embryos does not result in photoreceptor defects (9 of 9 for each group, data not shown). Based on these results, we conclude that the zebrafish *mikre oko* locus encodes a *dynactin 1* homolog. Although the mok^{m632} allele is predicted to encode a truncated polypeptide, we did not detect a shortened protein product on Western blots of extracts from homozygous mutant larvae or from adult heterozygotes (data not shown). The Mok polypeptide does not appear to be deposited maternally in a large

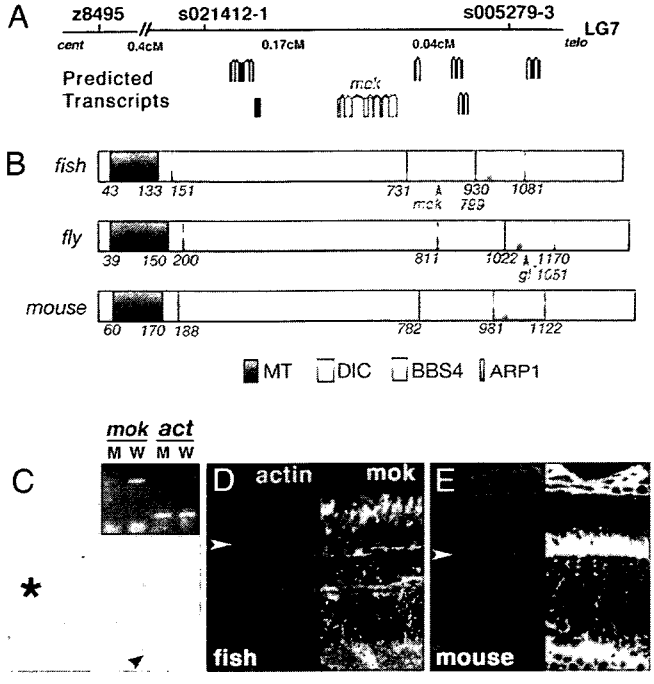

Fig. 2. Molecular characterization of the *mikre oko* (*mok*) gene. (*A*) Positional cloning of *mok*. (*B*) A schematic diagram of the zebrafish Mok polypeptide in comparison with its *Drosophila* and mouse homologs. In all three species, Mok polypeptide includes domains thought to bind microtubules (MT), dynein intermediate chain (DIC), actin-related protein 1 (ARP1), and BBS protein 4 (BBS4). In both the zebrafish and the fly, mutant alleles produce C-terminal truncations of the polypeptide (arrowheads). (*C*) A transverse section through the retina showing *mok* transcript distribution as evaluated by *in situ* hybridization. Arrowhead indicates the photoreceptor cell layer, and the asterisk indicates the lens. (*Inset*) RT-PCR reveals that the *mok* mRNA level is severely reduced in mok^{m632} mutant homozygotes, compared with their wild-type siblings. β-actin level (act) is unchanged. (*D* and *E*) Mok polypeptide distribution in zebrafish (*D*) and mouse (*E*) retinae. (*Right*) Anti-Mok antibody staining (red). (*Left*) F-actin distribution (blue). Staining is particularly prominent apical to the outer limiting membrane (arrowheads). In *D* and *E*, retinal pigmented epithelium is up.

quantity, because no obvious signal is present on Western blots from embryos at 2 h postfertilization (hpf) (data not shown). Consistent with its mutant phenotype, *mok* transcript is expressed in the eye, including the photoreceptor cell layer, at 3 dpf (Fig. 2*C*). Staining of zebrafish and mouse retinae with three different antibodies suggests that although present in the entire photoreceptor cytoplasm, the Mok polypeptide is enriched in the vicinity of cell junctions and in the inner segment (Fig. 2 *D* and *E* and data not shown). Staining of outer segments is either weak or absent.

Dynein Complex Regulates Nuclear Position in Vertebrate Photoreceptors. The Mikre oko polypeptide is a component of the dynactin complex, which consists of at least eight proteins and functions as a dynein regulatory subunit (8). The Mok involvement in nuclear positioning could be mediated either via the dynactin complex or by an independent mechanism. In the first case, the disruption of dynactin function by other means would also result in nuclear mispositioning. To test whether or not this is the case, we cloned another dynactin component, the zebrafish *p50/dynamitin* gene. In several experimental systems, the overexpression of p50 causes a dissociation of the dynactin complex and consequently blocks its function (9, 10). We took advantage of this observation and overexpressed *p50/dynamitin* in zebrafish photoreceptors by introducing a heat-shock-inducible DNA construct into zebrafish embryos and inducing its expression during photoreceptor differentiation at 2–3 dpf. Similar to mok^{m632} mutation, *p50/dynamitin* overexpression, but not the treatment with an empty vector, results in the mispositioning of photoreceptor nuclei, which in the most extreme cases translocate into the outer plexiform layer [Fig. 3*B* (compare with Fig. 3*A*, $P < 0.0003$)]. The zebrafish photoreceptors are well differentiated and functional by 3 dpf. To determine whether the dynein/dynactin complex maintains nuclear position in morphologically mature cells, we applied a series of heat shocks between 4.5 and 5.5 dpf. These tests also produced an obvious basal displacement of nuclei ($P < 0.0004$, Fig. 3*C*). These observations, together with the analysis of the *mok* phenotype, provide strong evidence that the dynactin complex regulates nuclear position in the vertebrate eye.

Because of its central role in visual perception and in neurodegenerative disorders of the eye, the vertebrate photoreceptor cell has been the focus of intensive research. Despite these efforts, many aspects of photoreceptor cell biology remain poorly investigated. We decided to investigate further what genes in addition to *mok* and *p50* may be involved in the positioning of photoreceptor nuclei. The lissencephaly-1 (Lis1) protein is a dynein motor cofactor known for its involvement in human cerebral cortex disorders (11–13). We cloned two zebrafish *Lis1* homologs, *lis1a* and *lis1b*, which display 93% identity and 96% similarity to each other and are highly homologous to the mouse polypeptide (93% identity and 97% similarity for Lis1a). *In situ* hybridization shows that *lis1a* is enriched in photoreceptor cells (Fig. 3 *H* and *I*). To test its function, we performed antisense morpholino knockdown. A *lis1a* splice site-directed morpholino nearly completely eliminates the wild-type transcript until at least 48 hpf (SI Fig. 7*A* and *SI Text*). Because in both *Drosophila* and the mouse, loss-of-function mutations in Dlis-1/Lis1 result in embryonic lethality (12, 14), to ameliorate its early embryonic phenotype, we studied *lis1a* function in mosaic animals. We transplanted blastomeres from anti-*lis1a* morpholino-treated donor embryos into untreated host blastulae and evaluated nuclear position in donor-derived photoreceptor cells. Treatment with two different anti-*lis1a* antisense oligonucleotides but not with a control morpholino results in a shift of photoreceptor nuclei to more basal positions (Fig. 3 *D–G*; $P < 0.0002$ for SP morpholino; $P < 0.008$ for ATG). To confirm the validity of these results, we overexpressed the N-terminal region (amino acids 1–87) of Lis1a in photoreceptor cells. We refer to this polypeptide as N-lis1. This protein fragment is known to interfere with Lis1a dimerization, mediated by its N-terminal coiled-coil motif (11, 15). In agreement with morpholino knockdown data, the overexpression of Lis1a N-terminal region produces a basal displacement of photoreceptor nuclei [SI Fig. 5*E* (compare with SI Fig. 5*D* and graph in SI Fig. 5*F*, $P < 0.00002$)]. These results indicate that one or both *lis1* genes regulate nuclear position in photoreceptor cells.

Positioning of Cell Nucleus Requires Nuclear Envelope Components. In addition to motor machinery, the regulation of nuclear position must involve factors that anchor the nucleus to the motor apparatus. Several nuclear envelope components are required for the correct localization of nuclei in flies and nematodes. KASH-domain proteins in particular, including ANC-1, MSP-300, and Klarsicht, have been shown to control nuclear position in several tissues (reviewed in ref. 16). The KASH domain is thought to anchor polypeptides to the nuclear envelope, and thus it is likely that KASH family proteins mediate the attachment of nuclei to the cytoskeleton (reviewed in ref. 17). To investigate the role of KASH-domain proteins in vertebrate photoreceptors, we cloned partial sequences of four zebrafish Syne genes: *syne1a*, *syne1b*, *syne2a*, and *syne2b*. Interestingly, the expression of *syne2a* is highly enriched in the eye (Fig. 4 *A* and *B*), particularly in photoreceptor cells (Fig. 4 *C* and *D*). The overexpression of the C-terminal portion of Syne/ANC-1 proteins,

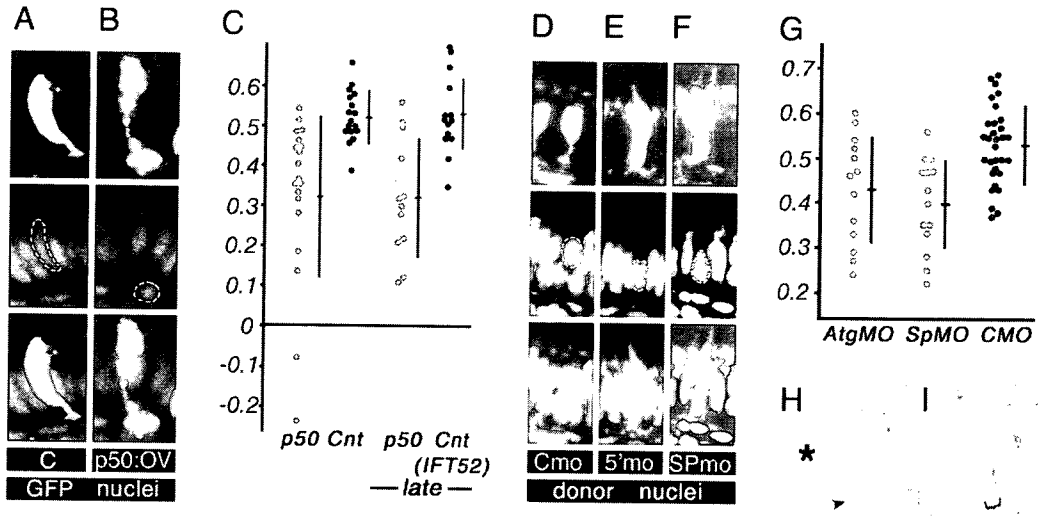

Fig. 3. Dynein complex function in nuclear positioning. (*A* and *B*) Mosaic overexpression of a control vector (*A*) or *p50* (*B*). Overexpressing cells are marked with GFP (green). In the most extreme cases (*B*), photoreceptor nuclei (blue) are displaced into the outer plexiform layer. (*C*) The distribution of nuclear positions in cells expressing *p50* vector (red dots), a control empty vector (black dots, center), or a control *ift52* overexpression vector (black dots, rightmost graph). (*D–F*) YoPro staining of cell nuclei (green) in genetically mosaic retinae, containing cells (red) derived from donor embryos treated with a control morpholino (*D*), anti-*lis1a* ATG (5′) morpholino (*E*), or anti-*lis1a* splice site (SP) morpholino (*F*). (*G*) Both ATG and SP morpholinos produce a statistically significant basal displacement of photoreceptor nuclei. (*H* and *I*) *In situ* hybridization result showing that *lis1a* is expressed in wild-type photoreceptors. (*A*, *B*, and *D–F*) (*Top*) Tracer labeling of cell somata in which nuclear positioning was evaluated (red for dextran tracer, green for GFP). (*Middle*) Nuclear staining (blue for ToPro-3, green for YoPro). (*Bottom*) Superimposed images from above; apical is up. (*H* and *I*) Arrowhead (*H*) and bracket (*I*) indicate the photoreceptor cell layer. Graphs in *C* and *G* are plotted as described in Fig. 1 legend. Asterisk indicates the lens.

a region highly conserved between vertebrate and invertebrate Syne/ANC-1 genes (Fig. 4*H*), is thought to act in a dominant negative manner (18, 19). To test the function of zebrafish *syne2a* in nuclear positioning, we overexpressed its KASH domain (69 C-terminal amino acids, we refer to this polypeptide as C-Syne2a) using a heat-shock promoter. This treatment produces a basal displacement of photoreceptor nuclei [Fig. 4 *G–G″* (compare with Fig. 4 *F–F″*); graph in Fig. 4*E*, $P < 0.000008$)]. To verify this result, we performed a knockdown of *syne2a* function, using a splice site-directed morpholino. This reagent eliminates the wild-type *syne2a* transcript nearly completely until at least 2 dpf (SI Fig. 7*B* and *SI Text*). Again in this case, photoreceptor phenotype was analyzed in mosaic animals. *syne2a* knockdown also causes a basal displacement of nuclei (Fig. 4*E*, $P < 0.0098$). These results indicate that *syne* family proteins function in the positioning of vertebrate photoreceptor nuclei, possibly by providing a mechanical link to motor complexes.

Nuclear Mispositioning Is Accompanied by a Decreased Photoreceptor Survival. Because many abnormalities of the outer segment structure and function lead to a photoreceptor loss (20), we hypothesized that nuclear positioning defects will have a similar outcome. To test whether this is the case, we interfered with the functions of either the dynein motor or nuclear envelope by overexpressing p50, N-lis1, and C-Syne2a polypeptides. Transposon-based Tol2 vector was used to produce expression in a large number of retinal cells, and the use of a heat-shock promoter allowed us to control the timing of expression (SI Fig. 8) (21). To test whether the mispositioning of photoreceptor nuclei is associated with a decreased survival, we induced the expression of p50, N-lis1, and C-Syne2a by heat-shocking larvae either shortly after photoreceptor formation at 48, 60, and 72 hpf, or after photoreceptor cells are fully differentiated and functional at 120, 132, and 144 hpf. In the first case, photoreceptor phenotype was analyzed at 4 and 6 dpf, and in the second case, photoreceptor phenotype was analyzed at 6, 7, and 8 dpf. In all cases, the interference with dynein complex function or *syne2a* resulted in a decreased percentage of surviving photoreceptor cells. The result was statistically significant for all N-lis1 and C-Syne2a overexpression tests and in two tests involving p50 (SI Fig. 8*F*). In contrast to photoreceptors, the percentage of ganglion cell layer neurons relative to the number of inner nuclear layer cells did not display consistent changes. The overexpression of each of three constructs resulted in a basal displacement of photoreceptor nuclei at 8 dpf (SI Fig. 8*G*) but did not affect the localization of synaptic markers, PMCA and syntaxin 3 (data not shown). Cell clone sizes were not obviously affected by overexpression experiments, as compared with control overexpression of GFP (SI Fig. 8*F*). These results indicate that the mispositioning of photoreceptor cell nuclei is accompanied by a decreased viability of photoreceptor cells.

Dynein Motor Functions in Apical Localization of BBS4. Mosaic analysis revealed that in contrast to nuclear position, several key aspects of apico-basal polarity remain intact in *mok* mutant cells (Fig. 1). To test whether nonautonomous aspects of *mok* function regulate photoreceptor polarity and may be the primary cause of cell degeneration, we stained *mok* mutant retinae with antibodies that recognize cell junction components, ZO-1, cortactin, and β-catenin, as well as with antibodies directed to apical membrane determinants: Crumbs, Nok, and Has (ref. 22 and references therein). During the initial stages of degeneration, *mok* mutant photoreceptors retain their normal elongated shape. None of the proteins tested appear to be mislocalized in mutant photoreceptors at this stage [SI Fig. 9*D* (compare with SI Fig. 9*C*) and data not shown]. The distribution of mitochondria, which localize apically in wild-type cells, also remains largely normal [SI Fig. 9*B* (compare with SI Fig. 9*A*)]. Finally, the localization of two synaptic markers, PMCA and SV2, is unaffected by the mok^{m632} phenotype (data not shown), suggesting that at later stages synaptic defects in mosaic retinae (Fig. 1 *J* and *K*) may be secondary to nuclear displacement.

In contrast to the above findings, the BBS4 polypeptide does not properly localize in *mok* mutant photoreceptors at stages preceding the loss of elongated morphology. BBS4 is a pericentriolar protein involved in the BBS, a human disorder characterized by photoreceptor loss, and consequently blindness (recently reviewed in ref. 23). In wild-type animals, anti-BBS4 antibodies detect small particles in the vicinity of photoreceptor cilia (SI Fig. 9 *E* and *G*). This staining is severely reduced in *mok* mutant photoreceptors, before their loss of elongated morphology (SI Fig. 9*F*). Blocking of *lis1a* function, using a low dose of morpholino oligonucleotides, also results in the loss of BBS4 staining from the apical termini of photoreceptors [SI Fig. 9*H* (compare with SI Fig. 9*G*; graph in Fig. 4*I*, $P < 0.000005$)]. These data indicate that in addition to its role in nuclear positioning,

the *mok* gene, and most likely the entire dynein motor complex, functions in the apical localization of at least some pericentriolar proteins. Mutations in this mechanism may be responsible for some forms of BBS.

Discussion

The vertebrate photoreceptor is one of the best-studied cells of the nervous system. Yet mechanisms that regulate its morphogenesis are poorly understood. Based on genetic evidence, here we propose a model of a mechanism that determines a key feature of photoreceptor morphology, nuclear position. This model stipulates that nuclear position in vertebrate photoreceptor cells is regulated by the dynein motor complex, which interacts directly or indirectly with nuclear envelope components (Fig. 4*J*). Importantly, our data suggest that the proper function of this mechanism is necessary for cell viability. Genetic defects in 50–100 loci are known to produce photoreceptor loss and blindness in humans and other vertebrates (for a recent review, see ref. 24). Nearly all of these genetic defects predominantly or exclusively affect the structure or the function of the photoreceptor outer segment. To our knowledge, the *mok* mutation provides the first example of a sensory neuron loss associated with a nuclear positioning phenotype. It is important to note, however, that *mok* photoreceptor loss also involves cell nonautonomous components (2). This aspect of the *mok* phenotype is unlikely to be mediated via nuclear positioning aberrations and may involve defects in cell–cell interactions mediated via cell junctions of the outer limiting membrane or, less likely, synaptic termini.

The nucleus is a bulky organelle that in many cases occupies a substantial fraction of cell volume. In neurons, cell somata are frequently almost entirely occupied by the nucleus, and it is the nuclear position that defines cell body. The regulation of nuclear position is thus a mechanism that contributes to tissue patterning in neuronal formations. The retina alone provides many examples of cells that display nonrandom nuclear positions. For example, although Muller glia span the entire thickness of the retina, their nuclei are positioned in the inner portion of the inner nuclear layer (see, for example, ref. 25). Similarly, cone nuclei are consistently located apical to rod nuclei (26). Experiments presented in this manuscript reveal a mechanism that regulates nuclear position in the photoreceptor cell layer of the retina. Similar mechanisms may be functional in other cell classes: glia and bipolar neurons, for example. Alternatively, forces that do not involve microtubule-based motors may also regulate nuclear position in other cells. Further studies of these mechanisms may be a source of important insights into the patterning of multicellular tissues.

Materials and Methods

Animals. The maintenance and breeding of zebrafish strains and staging of embryonic development were performed as described previously (27, 28). All animal protocols were approved by the MEEI animal care committee. Embryos were observed by using an Axioscope microscope (Zeiss, Thornwood, NY) or a Leica (Deerfield, IL) MZ12 dissecting scope.

Mosaic Analysis. Genetically mosaic animals were generated as described in ref. 29. Cells were transplanted into wild-type hosts from the progeny of crosses between mok^{m632} heterozygotes or from embryos injected with morpholino oligonucleotides. To distinguish mutant donor embryos, we isolated their DNA at 24 hpf and PCR-amplified the genomic fragment containing the mok^{m632} mutation, using the following two primers: CACACATCGTCAACTATTCCT and TTGTACCTGCTCCACTGCTT. The presence of mutation was determined by sequencing. Additional details can be found in *SI Text*.

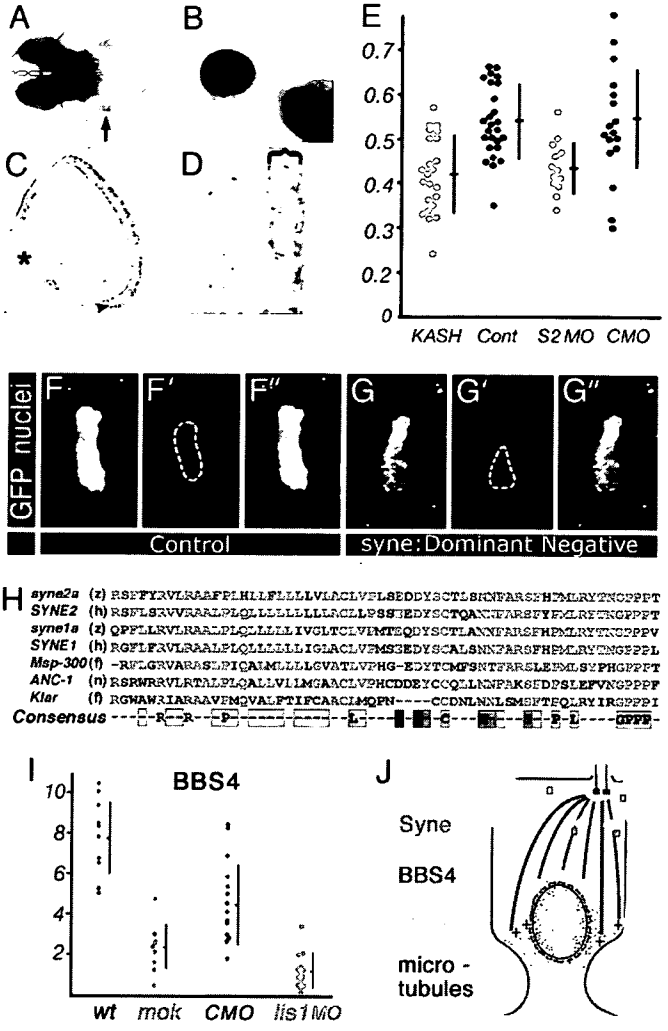

Fig. 4. The function of *syne2a* in nuclear positioning. (*A* and *B*) Dorsal (*A*) and lateral (*B*) views of PTU-treated zebrafish embryos at 50 and 72 hpf, respectively. Arrows indicate the pectoral fin. *syne2a* expression is strongly elevated in the eye. (*C* and *D*) Transverse sections through the zebrafish retina showing *syne2a* transcript expression detected by *in situ* hybridization. The photoreceptor cell layer is indicated with an arrowhead in *C* and with a bracket in *D*. (*E*) The distribution of nuclear positions in cells expressing dominant negative *syne2a* vector (KASH, red dots) or a control empty vector (Cont, black dots) (left side of the graph) and cells treated with an anti-*syne2a* morpholino (S2, red dots) or a control morpholino (CMO, black dots) (right side of the graph). The positions of nuclei are calculated as defined in Fig. 1. (*F–F''* and *G–G''*) Examples of data used to plot the distribution of nuclear positions in *E* in cells overexpressing a control vector (*F*) or a dominant negative *syne2a* (*G*). (*F* and *G*) GFP staining of cells in which nuclear positioning was evaluated. (*F'* and *G'*) Nuclear staining (ToPro-3). (*F''* and *G''*) Superimposed images; apical is up. (*H*) The alignment of KASH domains from two zebrafish *syne* genes to human sequences, and to sequences of invertebrate genes: Msp-300, ANC-1, and Klarsicht. Conserved residues are in red. The consensus sequence is color-coded as follows: magenta, nonpolar amino acids; blue, acidic; green, polar; yellow, basic. Species designations are as follows: z, zebrafish; h, human; f, fly; n, nematode. (*I*) The ratio of BBS4-positive particles to the number of cell somata in wild-type and *mok* photoreceptors (right side of the graph). The ratio of BBS4-positive particles to the number of basal bodies in *lis1a* morphants, and in control morpholino (CMO)-treated animals (left side of the graph). Each dot represents a separate retina. (*J*) A model of the mechanism that positions nuclei in vertebrate photoreceptors. The interaction of dynein with Syne polypeptide is hypothetical.

Cryosectioning and Immunohistochemistry. Sectioning and immunohistochemistry were performed as described in ref. 29. Sources of antibodies are provided in *SI Text*. We note that

antibody detection of Mok polypeptide in zebrafish is complicated because two Dynactin 1 genes are expressed in zebrafish retina. The antibodies that we use may recognize both. To evaluate BBS4 staining, the average thickness of the outer nuclear layer was estimated for each image, and one-fifth of that thickness from the apical margin of the outer nuclear layer was used to determine the area where staining would be examined. BBS-positive particles in this area were counted, and their ratio to the number of cell somata (stained by the Zpr-1 antibody) or to the number of basal bodies (stained by γ-tubulin antibody) was calculated.

Positional Cloning. A map cross was set up between heterozygous G_0 carriers of the *mok*^{m632} allele (AB genetic background) and wild-type WIK strain homozygotes. To determine *mok* position in the genome, we used a panel of 1,200 F_2 diploid embryos obtained via incrossing of F_1 animals. Genotyping of DNA polymorphisms was performed as described in ref. 3. To clone the full-length zebrafish *mok* cDNA, human and mouse *dynactin 1* coding sequences were obtained from the National Centre for Biotechnology Information public database and used to search the whole-genome zebrafish shotgun sequence database (Sanger Center, Cambridge, U.K.) with a homology search program, BLASTP. Based on partial sequences obtained in this manner, RT-PCR was performed to clone the full-length gene transcript, using conditions described in ref. 3.

Knockdown and Phenotypic Rescue. Morpholino-modified oligonucleotides (morpholinos; sequences provided in *SI Text*) were injected into wild-type AB embryos as described in ref. 28. To determine BBS4 distribution in *lis1* morphants, a mix of *lis1a*-ATG and *lis1a*-SP morpholinos (1.5 mg/ml each) was injected into embryos. In all other experiments, 3.0 mg/ml (1.5–2 nl) of each morpholino was injected separately. To rescue the mutant phenotype, the full-length *mikre oko* coding sequence was amplified by using the primers CAGTTCAGACGGCGGTGGGCG and TTTACGTCATGAGCAGGTGGT and cloned into the pXT7 vector (figure 1 in ref. 28). Messenger RNA was generated by using standard protocols and injected into embryos at the one cell-stage. Embryos were collected at 3.5 dpf, and their tails were removed, digested in a lysis buffer, and genotyped as above. After genotype determination, the anterior part of each embryo was cryosectioned, and sections were stained with the Zpr1 antibody and the Yo-Pro-1 nuclear stain as above.

Heat-Shock Overexpression. The following genes or gene fragments were used in overexpression studies: the N terminus of *lis1a* (first 87 aa), the KASH domain of *syne2a* (69 C-terminal aa), the entire coding region of *p50/dynamitin*, and the entire coding region of *ift52* (3) (used as a control in *p50* overexpression; Fig. 3*C*). Relevant DNA fragments were cloned into a heat-shock promoter driven zebrafish expression vector pXT7-HS (28). To monitor the distribution of DNA upon injection into embryos, overexpression constructs were mixed with pXT7-HS-GFP expression vector DNA in the 3:1 ratio. Linearized vector DNA was injected into one-cell stage embryos as described in ref. 28. Unless stated otherwise, heat-shock treatments (1 h each, at 38°C) were performed at 48, 60, and 70 hpf. For *p50*, heat shocks were also applied at 4, 4.5, and 5 dpf. Embryos were collected at 4 or 6 dpf and processed for antibody staining as above. Staining was performed on whole embryos, using an anti-GFP rabbit antibody (1:2,000; Clontech, Palo Alto, CA) in 10% goat serum in PBS Tween-20 overnight at 4°C. Embryos were embedded in JB-4 resin and sectioned, and sections were stained with To-Pro-3 nuclear dye (1:8,000; Molecular Probes, Eugene, OR).

***In Situ* Hybridization.** Partial sequences of relevant genes were amplified by RT-PCR, cloned into the pCR-II vector (Invitrogen, Carlsbad, CA), and sequenced. RNA probe synthesis, *in situ* hybridization, washes, and signal detection were carried out by using standard protocols as described in ref. 30. After hybridization, embryos were embedded in JB4 resin (Polysciences, Warrington, PA) and sectioned at 8 μm. Additional details are in *SI Text*.

We thank Drs. K. T. Vaughan (University of Notre Dame, Notre Dame, IN) and B. B. Vallee (Worcester Foundation for Biomedical Research, Worcester, MA) for a p150 antibody; Drs. Vihtelic and Hyde (University of Notre Dame) for anti-opsin antibodies; Dr. Nico Katsanis (The Johns Hopkins University, Baltimore, MD) for the anti-BBS4 antibody; and Drs. Pignoni, Dryja, Zon, Katsanis, and Heller for providing comments on earlier versions of this manuscript. This work was supported by a Knights Templar Pediatric Ophthalmology research grant (to M.T.), National Eye Institute Award RO1 EY016859 (to J.M.), and National Eye Institute Core Grant EY14104.

1. Malicki J, Neuhauss SC, Schier AF, Solnica-Krezel L, Stemple DL, Stainier DY, Abdelilah S, Zwartkruis F, Rangini Z, Driever W (1996) *Development (Cambridge, UK)* 123:263–273.
2. Doerre G, Malicki J (2001) *J Neurosci* 21:6745–6757.
3. Tsujikawa M, Malicki J (2004) *Neuron* 42:703–716.
4. Pugh E, Lamb T (2000) in *Handbook of Biological Physics* (Elsevier, Amsterdam), Vol 3, pp 183–255.
5. Mansergh F, Orton N, Vessey J, Lalonde M, Stell W, Tremblay F, Barnes S, Rancourt D, Bech-Hansen T (2005) *Hum Mol Genet* 14:3035–3046.
6. Swaroop A, Swaroop M, Garen A (1987) *Proc Natl Acad Sci USA* 84:6501–6505.
7. Holzbaur EL, Hammarback JA, Paschal BM, Kravit NG, Pfister KK, Vallee RB (1991) *Nature* 351:579–583.
8. Holleran EA, Karki S, Holzbaur EL (1998) *Int Rev Cytol* 182:69–109.
9. LaMonte BH, Wallace KE, Holloway BA, Shelly SS, Ascano J, Tokito M, Van Winkle T, Howland DS, Holzbaur EL (2002) *Neuron* 34:715–727.
10. Echeverri CJ, Paschal BM, Vaughan KT, Vallee RB (1996) *J Cell Biol* 132:617–633.
11. Tai CY, Dujardin DL, Faulkner NE, Vallee RB (2002) *J Cell Biol* 156:959–968.
12. Swan A, Nguyen T, Suter B (1999) *Nat Cell Biol* 1:444–449.
13. Xiang X, Osmani AH, Osmani SA, Xin M, Morris NR (1995) *Mol Biol Cell* 6:297–310.
14. Hirotsune S, Fleck MW, Gambello MJ, Bix GJ, Chen A, Clark GD, Ledbetter DH, McBain CJ, Wynshaw-Boris A (1998) *Nat Genet* 19:333–339.
15. Ahn C, Morris NR (2001) *J Biol Chem* 276:9903–9909.
16. Starr DA, Fischer JA (2005) *BioEssays* 27:1136–1146.
17. Starr DA, Han M (2003) *J Cell Sci* 116:211–216.
18. Starr DA, Han M (2002) *Science* 298:406–409.
19. Grady RM, Starr DA, Ackerman GL, Sanes JR, Han M (2005) *Proc Natl Acad Sci USA* 102:4359–4364.
20. Li T (2001) *Trends Mol Med* 7:133–135.
21. Kawakami K, Takeda H, Kawakami N, Kobayashi M, Matsuda N, Mishina M (2004) *Dev Cell* 7:133–144.
22. Omori Y, Malicki J (2006) *Curr Biol* 16:945–957.
23. Blacque OE, Leroux MR (2006) *Cell Mol Life Sci* 63:2145–2161.
24. Hartong DT, Berson EL, Dryja TP (2006) *Lancet* 368:1795–1809.
25. Peterson RE, Fadool JM, McClintock J, Linser PJ (2001) *J Comp Neurol* 429:530–540.
26. Raymond P, Barthel L, Rounsifer M, Sullivan S, Knight J (1993) *Neuron* 10:1161–1174.
27. Kimmel CB, Ballard WW, Kimmel SR, Ullmann B, Schilling TF (1995) *Dev Dyn* 203:253–310.
28. Malicki J, Jo H, Wei X, Hsiung M, Pujic Z (2002) *Methods* 28:427–438.
29. Avanesov A, Malicki J (2004) *Methods Cell Biol* 76:333–384.
30. Oxtoby E, Jowett T (1993) *Nucleic Acids Res* 21:1087–1095.

34. ロドプシントランスジェニックウサギ作成の試み

近藤峰生[1)]、坂井隆夫[1)]、米今敬一[1)]、栗本幸英[1)]、子安俊行[1)]、宮田健太郎[1)]
西沢祐治[2)]、臼倉二郎[3)]、不二門尚[4)]、田野保雄[4)]、寺崎浩子[1)]
([1)] 名古屋大、[2)] 名古屋大細胞生物学、[3)] 名古屋大エコトピア研究所、[4)] 大阪大)

研究要旨 我々は、NZW 種ウサギにロドプシン変異遺伝子を導入することによって進行性網膜変性ウサギの作成を試みた。ロドプシン遺伝子を含むウサギ BAC クローンを抽出し、ロドプシン遺伝子の 347 番目の Pro を Leu に置換してウサギの受精卵に注入した。その結果合計 10 匹のファウンダーが得られ、そのうち 6 匹からトランスジェニック陽性 F1 個体が得られた。この 6 つのラインのうち少なくとも 3 ラインは網膜電図と網膜組織で進行性の網膜変性所見を示し、その変性スピードは transgene 発現量にほぼ比例していた。ウサギは眼球構造でヒトと異なる点はあるが、眼球サイズはヒトに近く、また扱いやすい動物である。細胞シート移植や人工視覚などの実験に用いる動物モデルとして役立つ可能性がある。

A. 研究目的

人工視覚、栄養因子除放カプセル移植、細胞シート移植のような治療の実験では、眼球のサイズがよりヒトに近い動物モデルが必要になる。欧米では網膜色素変性に対する新規治療法の開発に中動物-大動物のモデルが必要であると認識され、自然発症の RP モデル（ネコ、イヌなど）の系統樹立や大型トランスジェニック動物（ブタなど）の作成のプロジェクトが試みられてきた。しかし本邦にはラットより大きい RP モデルが存在しない。

そこで今回我々は、網膜色素変性の原因となる遺伝子変異の 1 つをウサギに導入することにより、進行性の網膜変性をおこす中型動物モデルの作成を試みたので報告する。

B. 研究方法

国際的に中型実験動物として広く用いられている NZW 種ウサギの遺伝子ライブラリーからロドプシン遺伝子の全領域を含む BAC クローン（100-150kb のゲノム断片）を抽出し、ロドプシン遺伝子の 347 番目の Pro を Leu に置換した BAC transgene を作成し、ウサギの受精卵に注入した。その後偽妊娠処理した 17 匹の雌ウサギに合計 456 個の受精卵を移植した。

（倫理面への配慮）

全ての実験は名古屋大学動物実験委員会の承認を得て行なった。全ての実験は ARVO の動物実験規定に従った。

C. 研究結果

移植した 17 匹中 12 匹が妊娠し、合計 80 匹の産仔を得た。80 匹中 12 匹（2 匹は死亡）

が DNA 検査にてトランスジェニック陽性であることがわかった。得られた 10 匹のファウンダーを生殖期（約 12 週）まで飼育して交配させ、F1 世代を得た。10 個のラインのうち 6 つのラインでトランスジェニック陽性 F1 個体を得た。この 6 ラインのうち 3 ライン（#7, #8, #16）が網膜電図と組織学検査によって進行性の網膜変性をおこしていることがわかった。定量的リアルタイム RT-PCR 法によって、最も変性の速い#7 における変異遺伝子の発現量（対正常ロドプシン）は 50%程度であることを確認した。また変異遺伝子の発現量は、網膜変性のスピードにほぼ比例していた。

興味深いことに、この Tg ウサギの変性早期（3 か月）では、視細胞電位（a 波）や双極細胞の電位（b 波）は正常より明らかに減弱しているにもかかわらず、網膜内層機能を反映する網膜電図の律動様小波の一部は正常よりも大きい hyper-normal を示していた。

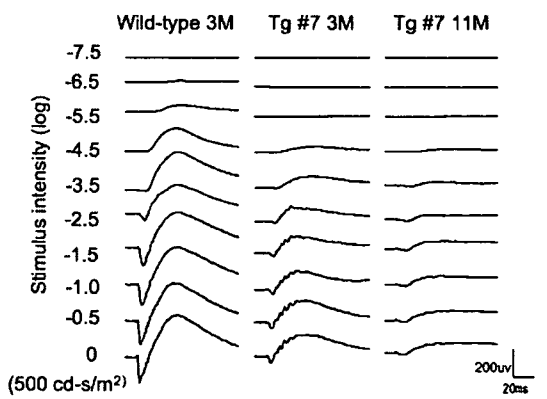

図 1　正常ウサギとトランスジェニックウサギから記録した網膜電図

D．考察

これまで本邦ではラットより大きな動物の網膜変性モデルの系統が樹立されていなかった。今回我々は、実際に日本人の網膜変性患者にも確認されているロドプシン P347L 変異をウサギに導入し、ウサギ種で進行性の網膜変性モデルを作成することに成功した。

今回のウサギで確認した律動様小波の hyper-normal については、我々は同様の現象を実際の RP 患者の黄斑部局所網膜電図で見いだしている（IOVS, 2007）。現在はこの Tg ウサギにみられる網膜中内層の二次的変化を免疫組織学的に検証中の段階である。

E．結論

今回我々は、ウサギ種で初めて進行性の網膜変性動物を作成することに成功した。ウサギの眼の構造（特に網膜血管）はヒトのそれと若干異なるが、ヒトの眼球に近い大きな眼球を有しており、今後網膜色素変性の治療研究に有用な動物モデルになる可能性がある。

F．健康危険情報

なし

G．研究発表

1．論文発表

1. Ikenoya K, Kondo M et al: Preservation of Macular Oscillatory Potentials in Eyes of Patients with Retinitis Pigmentosa and Normal Visual Acuity. Investigative Ophthalmology & Visual Science 48: 3312-3317, 2007

2．学会発表

1. Kondo M, Ikenoya K et al: Preservation of Macular Oscillatory

Potentials in Eyes of Patients with Retinitis Pigmentosa and Normal Visual Acuity. Annual Meeting of the Association for Research in Vision and Ophthalmology. Florida, USA. May 9, 2007.

H. 知的財産権の出願・登録状況

1. 特許取得

なし

2. 実用新案登録

なし

3. その他

なし

I. 参考文献

1. Petters RM et al: Genetically engineered large animal model for studying cone photoreceptor survival and degeneration in retinitis pigmentosa. Nat Biotechnol. 15:965-970, 1997

35. 中型動物における視細胞障害モデルの作成

西田健太郎[1)]、瓶井資弘[1)]、近藤峰生[2)]、坂口裕和[1)]、不二門尚[1)]、田野保雄[1)]

([1)] 大阪大、[2)] 名古屋大)

研究要旨　有効な治療法のない網膜変性疾患に対して、本邦独自の人工網膜である、脈絡膜上経網膜電気刺激（STS）法を開発した。動物実験に引き続き、急性臨床試験を行い、失明した患者に擬似光覚が得られることを確認した。次に、最適な刺激パラメーターを決定するために、健常な動物ではなく、適応患者と類似した視細胞変性モデルが必要となってくる。これまで、マウス、イヌ、ブタなどの視細胞変性モデルは存在するものの、眼球が小さすぎたり、飼育施設の問題などがあり実験に適していない。そこで今回、有色家兎に対するベルテポルフィンと赤色 LED 光を用いた光障害モデルの作成を検討した。その結果、広範囲において視細胞を選択的に障害することに成功した。さらに、この障害部位に STS 法の刺激電極を埋植することにより、大脳皮質で電気的誘発電位（EEP）を測定することにも成功した。この結果は、有色家兎に対してベルテポルフィンと赤色 LED を用いた光照射で作成される視細胞障害モデルが、人工視覚の実験のための貴重な疾患モデルとなりえる可能性があることを示すものである。

A．研究目的

有効な治療法のない網膜変性疾患に対して、本邦独自の人工網膜である、脈絡膜上経網膜電気刺激（STS）法を開発した。動物実験に引き続き、急性臨床試験を行い、失明した患者に擬似光覚が得られることを確認した。次に、最適な刺激パラメーターを決定するために、健常な動物ではなく、適応患者と類似した視細胞変性モデルが必要となってくる。

これまで、マウス、イヌ、ブタなどの視細胞変性モデルは存在し、我々もマウスを使用した研究を行ってきた。しかし、眼球が小さすぎため、臨床応用のための多極チャンネルを有する刺激電極を埋設する実験に適していない。網膜変性イヌやブタは海外の研究施設で開発系統維持されており、入手が困難であるうえに、飼育条件を満たした研究施設の問題が残る。

今回、中型実験動物として扱いやすく、実験にも適していると考えられる有色家兎を用いて、ベルテポルフィンと赤色 LED を用いた光障害モデルの作成を検討した。もともと、ラットやマウスの光障害モデルの研究は多く、その障害のされ方が網膜色素変性症と類似していると報告されている。しかしながら、家兎の場合、ラットやマウスと比較すると非常に光に対しての耐性が強靭であり、同じような条件では視細胞の障害は起こらないことが知られている。そのため、今回は強力な光照射と光感受性物質のベルテポルフィンを用いることにより、

視細胞障害が出来ないか検討し、視細胞障害を生じることができた。また、このモデルにおいてSTS方式の電極で、大脳皮質で誘発電位（EEP）を誘導することに成功したので報告する。

B. 研究方法

対象：有色家兎（n=5）

方法：有色家兎(2.0-2.2kg)を0.5%トロピカミド・5%フェニレフリンにて散瞳し、持続点滴（2cc/h、ケタラール：キシラジン＝2：1）を用いて麻酔を行ったうえで、ベルテポルフィンを静脈投与し（0.47mg/kg)、5分後より赤色LED光源（MCEP-CR8　MORITEX社製、1cm:9.5mW/cm^2　図1）を眼前（角膜頂点より1mm程度）に固定し、3方向に対して合計90分間照射を行った。

照射前後に、眼底写真、蛍光眼底造影検査、網膜電図（全視野ERGと局所ERG）を測定し、照射後1か月の時点で照射部位にSTS方式の刺激電極を埋植し、大脳皮質でEEPを測定した。その後、眼球摘出を行い、4%パラホルムアルデヒドにて24時間固定し、凍結切片を作成し、HE染色を行った。

（倫理面への配慮）

ARVO動物実験の規定に準じて動物を取り扱い、最小限の苦痛で実験を行なった。

C. 研究結果

照射後1カ月の時点で、眼底写真ではVisual Streakを含む広範囲に網脈絡膜変性が認められ（図1)、蛍光眼底造影検査でも、その変性部位に一致した低蛍光な像が見られた（図2)。また、1ヶ月後の全視野ERGでは、a波、b波とも30～35%程度の振幅が減弱し（図3)、照射部位での局所ERGではフラットであった（図4)。局所ERGが認められなかった照射部位に、STS方式の刺激電極を埋植して電気刺激を行うことにより、EEPを誘発することに成功した(図5)。同部位での組織標本では、重症の網膜色素変性症患者の組織標本（図6）と同様に、視細胞層を含む網膜外層が消失し、網膜内層が維持されていた（図7)。

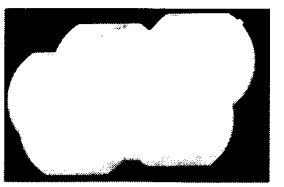

図1 照射後1か月の眼底写真 Visual Streakを含む広範囲に網脈絡膜変性を認める。

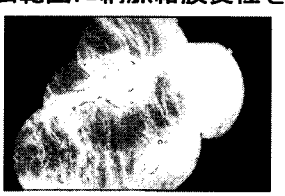

図2　照射後1カ月の蛍光眼底造影。図1の網脈絡膜変性に一致した範囲に低蛍光がみられる。

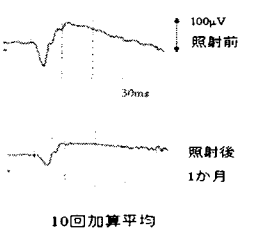

図3　照射前と照射後1か月の全視野ERG. a波、b波ともに3分の2程度に減弱した。

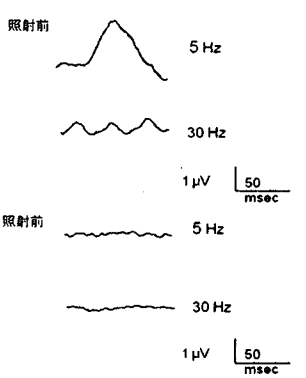

図4　照射前と照射後1か月の局所ERG.　照射前では、5Hz及び30Hzの光刺激で振幅が得られたが、照射後1カ月ではフラットであった。

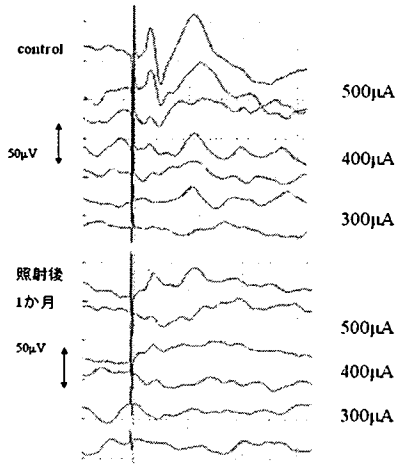

図 5　照射後 1 か月のコントロール眼と照射部位それぞれに STS 方式の刺激電極を入れたときの EEP 刺激条件は、Biphasic cathodic first duration 500μs。コントロール眼よりは小さいものの、照射眼でも EEP が誘発された。

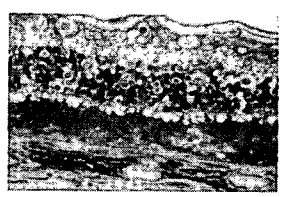

図 6 重症の色素変性患者の網膜の組織標本[1)] 外顆粒層をはじめ視細胞層が完全に消失しているが、網膜内層は維持されている。

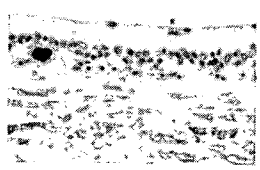

図 7　照射後 1 カ月の 400 倍の HE 染色　図 6 と同様に視細胞層、外顆粒層が完全に消失しているが、網膜内層は温存されている。

D．考察

ベルテポルフィンと赤色 LED を用いたモデルであるため、脈絡膜循環が障害されていると考えられる。家兎の場合は、網膜内層も脈絡膜循環で栄養されているために、照射後長期間経過を見た場合は、網膜内層まで障害される可能性がある。しかし照射後 1 カ月の時点では、組織学的にも網膜内層は温存されており、STS 方式の刺激電極により EEP を誘発できているので、照射後 1 カ月で実験に用いれば、人工視覚実験に有用な動物モデルとなりうると考えられた。

E．結論

今回我々は、ベルテポルフィンと赤色 LED を用いた光照射により、広範囲に有色家兎の視細胞を障害することができた。また、このモデルにおいて、STS 方式の刺激電極で EEP を誘発することに成功し、人工視覚実験に有用な動物モデルとなりうる可能性があることが示唆された。

F．健康危険情報

なし

G．研究発表

1．論文発表

なし

2．学会発表

なし

H．知的財産権の出願・登録状況

1．特許取得

なし

2．実用新案登録

なし

3．その他

なし

I．参考文献

1. Santos, et al: Preservation of the inner retina in retinitis pigmentosa. A morphometric Analysis. Arch Ophthalmol 115: 511-515, 1997

36. PEDFによる視細胞死の抑制とその作用機序に関する検討

村上祐介[1)2)]、池田康博[2)]、米満吉和[3)]、鬼丸満穂[1)]、向野利一郎[2)]、宮崎勝徳[2)]
中村　誠[4)]、矢部武士[5)]、井上誠[6)]、長谷川護[6)]、石橋達朗[2)]、居石克夫[1)]
([1)]九州大病理病態学、[2)]九州大、[3)]千葉大遺伝子治療学
[4)]神戸大、[5)]北里大生命科学、[6)]ディナベック㈱)

研究要旨　神経栄養因子PEDF（pigment epithelium-derived factor）は、網膜変性モデル動物における視細胞死を強力に抑制する。本研究ではその作用機序について検討した。ラット網膜由来細胞株R28において、PEDFは血清除去刺激によるR28のアポトーシスを抑制した。この細胞死は汎カスパーゼインヒビターであるZ-VAD-fmkでは抑制されなかったが、カスパーゼ非依存的なアポトーシス誘導因子であるAIFの発現抑制により有意に抑制された。血清除去刺激によりAIFはミトコンドリアから核内へ移行したが、PEDFの投与によりこの核内移行は著明に抑制された。網膜変性モデル動物であるRCSラットにおいても同様に、アポトーシスに陥った視細胞ではAIFの核内移行が観察された。さらに、SIVベクターを用いたPEDF遺伝子発現によりAIFの核内移行は著明に抑制され、5週齢のRCSラットにおいて視細胞のアポトーシスが有意に減少した。以上の結果より、AIFの核内移行は網膜変性における視細胞死に重要であると考えられた。PEDFを用いた網膜色素変性に対する視細胞保護遺伝子治療は、AIFの核内移行を標的とした理に適った治療法である可能性が示唆された。

A．研究目的

網膜色素変性は多数の遺伝子異常によって引き起こされる先天性遺伝性の疾患群で、最終的には視細胞にアポトーシスが誘導される。これまでに我々は、神経栄養因子であるPEDF（pigmentepithelium-derived factor）を網膜に遺伝子導入することで、視細胞のアポトーシスが抑制され、疾患モデルに対して治療効果が得られることを報告してきた。しかし、その作用機序については不明な点が多く、本研究ではその作用機序について検討した。

B．研究方法

培養細胞はラット胎仔網膜由来細胞株R28を用い、血清除去によりアポトーシスを誘導した。疾患モデル動物はRCSラットを使用し、サル由来レンチウイルス（SIV）ベクターを用いて網膜にPEDF遺伝子を導入した。カスパーゼ依存的経路の阻害にはZ-VAD-fmkを用いた。apoptosis-inducing factor（AIF）の細胞内局在は蛍光免疫染色法で検討し、その発現抑制にはsiRNAを用いた。

（倫理面への配慮）

実験は当該施設の動物実験委員会の承認を

得た後に Association for Research in Vision and Ophthalmology (ARVO)の規定に従って行った。動物の苦痛は最小限となるよう配慮した。

C. 研究結果

PEDF は血清除去刺激による R28 のアポトーシスに対して保護作用を示した。この細胞死は Z-VAD-fmk では抑制されなかったが、カスパーゼ非依存的なアポトーシス誘導因子である AIF の発現を抑制することで有意に抑制された。血清除去刺激により AIF はミトコンドリアから核内へ移行したが、PEDF の投与によりこの核内移行は著明に抑制された。RCS ラットにおいても同様に、アポトーシスに陥った視細胞では AIF の核内移行が観察された。さらに、SIV ベクターを用いた PEDF 遺伝子発現により AIF の核内移行は著明に抑制され、視細胞のアポトーシスは有意に減少した。

D. 考察

これまでに、網膜変性モデルにおいて、カスパーゼの活性を阻害しても視細胞死に変化がなかったことが報告されている。一方 AIF は、本検討に加え、別の遺伝子異常を有する rd1 マウスにおいても視細胞死に重要な役割を担うことが報告されており、網膜変性疾患の病態に共通する経路である可能性が考えられた。さらに、本検討により PEDF が AIF の核内移行を制御しアポトーシスを抑制することが明らかとなった。

E. 結論

AIF の核内移行は網膜変性における視細胞死に重要と考えられた。PEDF を用いた視細胞保護治療は AIF を標的とし、網膜変性に対する有用な治療法である可能性が示唆された。

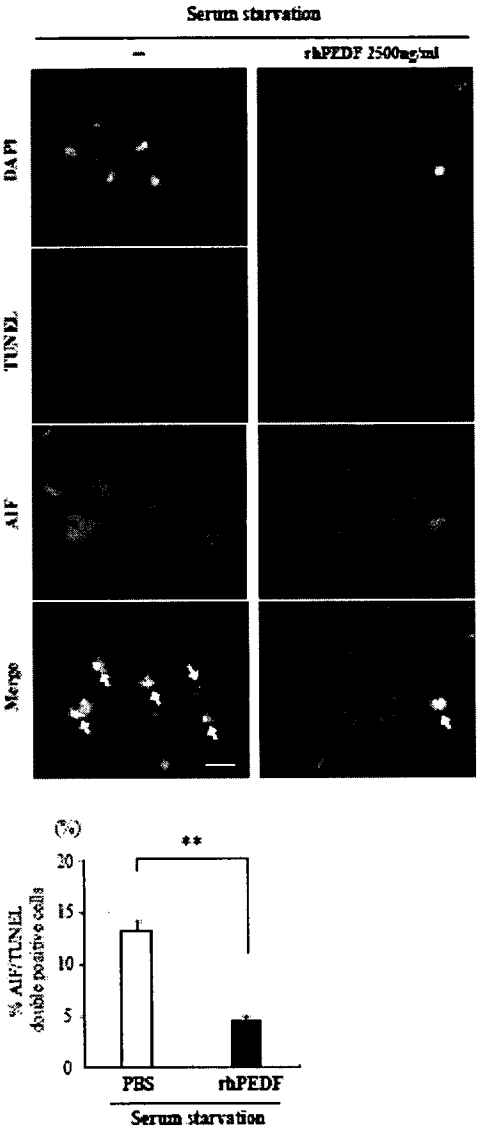

図1 PEDFは血清除去刺激後のAIFの核内移行を抑制し、アポトーシスを抑制する

F. 健康危険情報

なし

G. 研究発表

1. 論文発表

なし

２．学会発表

なし

H．知的財産権の出願・登録状況

１．特許取得

なし

２．実用新案登録

なし

３．その他

なし

I．参考文献

1. Ikeda Y et al: Simian immunodeficiency virus-based lentivirus vector for retinal gene transfer: a preclinical safety study in adult rats. Gene Ther 10(14):1161-1169, 2003
2. Miyazaki M et al: Simian Lentiviral vector-mediated retinal gene transfer of pigment epithelium-derived factor protects retinal degeneration and electrical defect in Royal College of Surgeons rats. Gene Ther 10(17):1503-1511, 2003
3. Sanges D et al: Apoptosis in retinal degeneration involves cross-talk between apoptosis-inducing factor and caspase-12 and is blocked by calpain inhibitors. Proc Natl Acad Sci USA 103(46):17366-17371, 2006